



Diosgenin Nanoparticles Competes Plain Diosgenin on Reviving Biochemical and Histopathological Alterations in DMBA Induced Rat Mammary Carcinoma via Modulating the AhR-Nrf-2 Signaling Cascades

Manobharathi Vengaimaran¹, Kalaiyarasi Dhamodharan¹ and Mirunalini Sankaran^{1*}

¹*Department of Biochemistry and Biotechnology, Faculty of Science, Annamalai University, Annamalai Nagar – 608 002, Tamil Nadu, India.*

Authors' contributions

This work was carried out in collaboration among all authors. All authors read and approved the final manuscript.

Article Information

DOI: 10.9734/JPRI/2021/v33i47A32998

Editor(s):

(1) Dr. Prem K. Ramasamy, Brandeis University, USA.

Reviewers:

(1) Mutaz Sabah Ahmeid, Ibsina University, Iraq.

(2) Dantew Bekele, Ambo University, Ethiopia.

Complete Peer review History: <https://www.sdiarticle4.com/review-history/76135>

Original Research Article

**Received 18 July 2021
Accepted 22 October 2021
Published 25 October 2021**

ABSTRACT

Background: Diosgenin, a steroidal saponin spotted as a primary ingredient in many traditional Chinese medicines, has sparked the attention of researchers owing to its multi-targeted cytotoxicity towards a multitude of cancers. Regrettably, its true potential was bounded by its impoverished physicochemical properties. In order to fully exploit its ability, we plan to fabricate diosgenin into nanoparticle by encapsulating with biodegradable polymer chitosan.

Aim: The current research intends to uncover the therapeutic potency of diosgenin encapsulated chitosan nanoparticles (DG@CS-NP) on 7,12dimethylbenz(a)anthracene (DMBA) induced rat mammary carcinoma by optimizing biochemical and histopathological modifications via attenuating Aryl hydrocarbon receptor (AhR) - nuclear factor erythroid-derived 2-related factors (Nrf-2) signaling.

Methodology: Breast cancer was induced with a single dose of DMBA (25 mg/kg b.wt). Orally supplied DG 10mg/kg b.wt. and DG@CS-NP 5 mg/kg b.wt to DMBA-induced tumor-bearing rats shortly after tumor onset. After the experimental period, biochemical and histopathological studies were performed using mammary tissue sections. Furthermore, architectural immunohistochemistry was used to reveal the expression of AhR and Nrf-2 in experimental rats. Additionally, diosgenin interactions with these proteins were also evidently confirmed by molecular docking analysis.

Result: We noticed that there is an elevated level of lipid peroxidative marker, phase-I detoxification enzymes, total cholesterol (TC), phospholipids (PL), triglycerides (TG), and free fatty acids (FFA) with boosted AhR expressions as well as diminished levels of enzymatic and non-enzymatic antioxidants and Phase – II detoxification enzymes with down-trodden Nrf-2 expressions in the mammary tissues of DMBA-induced rats. On the other contrary, oral dosing of DG@CS-NP 5 mg/kg b.wt, dramatically reverted them to near-normal tiers. Interestingly, molecular docking analyses also corroborate these insights by highlighting diosgenin's significant interactions with AhR and Nrf-2 targets.

Conclusion: As an outcome of our observations, we conclude that nano-encapsulation of diosgenin is a potent targeted therapeutic candidate posing a massive impact on breast cancer than plain diosgenin.

Keywords: Diosgenin; oxidative stress, detoxification enzymes; aryl hydrocarbon receptor; nuclear factor erythroid-derived 2-related factors; Mammary carcinogenesis.

1. INTRODUCTION

Breast cancer, the prime pervasive cancer amongst women and the second leading consequence of cancer mortalities [1]. Nowadays, environmental chemicals are increasingly accountable for approximately 75% of all cancers. The polycyclic aromatic hydrocarbons (PAHs), which are omnipresent in the environment, exist in the form of chemicals produced through the incomplete combustion of coal, gas, garbage, tobacco, and charbroiled meat, seems to be the preeminent genus of xenoestrogens, embroiled in the progression of breast cancer. An assessment of PAH-induced mammary carcinogenesis in rodents may offer a clear outline towards the intricate biochemical and molecular processes which drive the subtle reorientation of healthy cells into cancerous cells [2]. PAHs, such as 7,12-Dimethylbenz[a]anthracene (DMBA), a pluripotent carcinogen, elicits rat mammary carcinoma that firmly parallels human breast cancer because it aggressively metabolites with its ability to disrupt the DNA molecule, the pivotal point in carcinogenesis activation, through pursuing the metabolism by phase I and II xenobiotic-metabolizing enzymes (XMEs) which are sparked by the antioxidant response element (ARE) [3,4]. DMBA, a procarcinogen, demands oxidation to convert itself to the supreme carcinogenic diol epoxide metabolites, that are brought out by CYP1A1 and CYP1B1. These oxidation and reduction interactions often release immense amounts of free radicals, which tilt the redox balance in favour of the oxidizing agent,

culminating in oxidative damage, that performs a notable character in breast cancer. The sequential steps of reversal oxidative stress and persistent oxidative damage typically indicate the principle of biological degradation and the toxicity of such reactive oxygen species (ROS) on biomolecules. Cellular and organelle frameworks are immensely responsive towards such ROS attack, noted as lipid peroxidation [5]. Moreover, aryl hydrocarbon receptor (AhR), a cytosolic protein that could indeed be triggered by PAH, controls CYP1A1 and CYP1B1 expression. As like other PAHs, DMBA sticks and stimulates the AhR. Then, the activated AhR forms a heterodimer with aryl hydrocarbon receptor nuclear translocator, a nuclear transcription factor protein (ARNT). When the active heterodimeric AhR–ARNT complex attaches to a DNA sequence known as a dioxin or xenobiotic responsive element (DRE or XRE), transcription of genes encoding phase I enzymes arises [6]. AhR also elevates triglycerides (TG) amounts via rising the expression of a fatty acid transporter. In addition, oddities in the lipid tiers like total cholesterol (TC), phospholipids (PL), and free fatty acids (FFA) were also reported to be indicators of these metabolic disruptions [7]. Therefore, nuclear factor erythroid-derived 2-related factors (Nrf-2), a transcription factor, acts as an oxidative stress regulator and a principal activator of ARE, vital for cellular oxidative defence [8]. It mediates antioxidant enzymes superoxide dismutase (SOD), catalase (CAT), glutathione peroxidases (GPx), and non-enzymatic antioxidants such as reduced glutathione (GSH) and ascorbic acid, which

promptly curtail reactive oxygen species (ROS) released as by-products of phase I reactions and convert them to nontoxic physiological amounts. All of these volitional defensive modalities are satisfactory to compete with deleterious levels of xenobiotics. Thus, the intracellular chemical defence becomes dependent on a complex of stress-responsive genes, which have been the core target of countless cancerous investigations [9].

Recently, several natural bioactive compounds act as a stress antagonist with multifaceted therapeutic qualities, which were intensely explored owing to their antioxidant, antimutagenic, and anticarcinogenic impacts. Moreover, antioxidant and anti-radical features were being credited to its output of plants in an attempt to aid themselves in grappling with oxidative stress scenarios under inappropriate *in vitro* and *in vivo* growth environments that may entail the contribution of hydroxyl or thiol group-containing compounds [10]. In particular, Saponins gains much attraction with their ability to improve the expression and activation of the targeted downstream antioxidants such as SOD, CAT, GPx, GSH, etc, by provoking Nrf-2 pathways [11]. Favourably, Diosgenin, a natural steroidal saponin, shows potent anticancer activity by inhibiting peroxidation reactions and marker enzymes by enhancing the inherent antioxidant defence mechanism [12]. Amidst its versatile therapeutic effects, diosgenin's clinical use is hampered by diminished bioavailability and limited water solubility. Moreover, biopolymeric nanoparticle encapsulation were often employed as drug delivering vehicles because they offer a multitude of outcomes covering the stable delivery of non-water-soluble substances. [13,14]. In order to fully exploit its ability, we formulate diosgenin encapsulated nanoparticles with chitosan as a biodegradable carrier. We therefore undertook this study to quantify the impact of diosgenin encapsulated chitosan nanoparticles (DG@CS-NP) on revitalizing biochemical and histopathological alterations in DMBA-induced rat mammary carcinoma via modulating AhR-Nrf-2 signaling pathway.

2. MATERIALS AND METHODS

2.1 Chemicals

Diosgenin, 7,12-dimethylbenz(a)anthracene (DMBA), Chitosan, sodium tripolyphosphate (TPP) were purchased from Sigma-Aldrich

Co.Ltd. Thiobarbituric acid (TBA), phenazine methosulphate (PMS), nitroblue tetrazolium (NBT), reduced glutathione (GSH) and dimethyl sulphoxide (DMSO) were purchased from Himedia. Primary antibodies for AhR and Nrf-2 were purchased from Santa Cruz Biotechnology (Santa Cruz, CA, USA). All additional chemicals were of analytical grade and purchased from local commercial outlets.

2.2 Animal Model

Female Sprague-Dawley rats (weighed 130 – 150 g) were procured from Biogen Laboratory Animal Facility, Bangalore, India. The experiment was carried out at the Central Animal House, Rajah Muthiah Medical College and Hospital, Annamalai University, Chidambaram, India. Rats were granted a week to acclimatize before the experiment began. The animals were housed in six spacious polypropylene cages lined with husk under standard laboratory conditions: temperature (27 ± 2 °C) and humidity ($55\pm 5\%$) with a 12-hour light/dark cycle. The rats were fed with standard animal feed and water ad libitum during the entire period of the study.

2.3 Tumour Induction

Female Sprague-Dawley rats were administered with DMBA (25 mg/kg body weight), a dose intended to make sufficient tumor incidence in the control group over the course of the study. The DMBA was dissolved in a 1 mL emulsion of sunflower oil (0.75 mL) and physiological saline (0.25 mL) [15].

2.4 Experimental Design

Group I rats will be served as the control group. During the first week of the experiment, Groups II - V will receive a single subcutaneous injection of 25mg/kg b.wt DMBA. After 7 weeks, Groups III and IV will be medicated with DG and DG@CS-NP at 10mg/kg b.wt and 5mg/kg b.wt, respectively, thrice a week (21 days), orally. Groups V and VI will be supplied with CS-NP and free DG@NP at the concentrations of 5 mg/kg b.wt, thrice a week, orally. The dosage applied in the current study are based on earlier analyses [16,17]. The experiment was terminated after 14 weeks, and all rats were sacrificed by administering ketamine at a dose of 60 mg/kg b.wt. The mammary tissue was quickly dissected, washed thoroughly using ice-cold saline. Then a part of the tissue was homogenized in 0.1M Tris hydrochloric acetic

acid buffer (pH=7.4) before being centrifuged at 3000g for 10 minutes at 40°C. The supernatant was collected and processed to assess specific biochemical parameters. The remaining tissues were preserved using 10% formalin for histochemical analyses.

2.5 Measurement of Tumour Incidence and Tumour Volume

The frequency of tumors per rat was used to estimate tumor multiplicity. The tumor volume was ascertained using the formula $\frac{4}{3} \pi r^3$, where r indicates the diameter of the tumor in millimetres. The mean tumor burden was evaluated by multiplying the number of tumors in each group by the mean tumor volume in millimetre.

2.6 Biochemical Assays

2.6.1 Assessment on lipid peroxidation

The concentrations of thiobarbituric acid reactive substances (TBARS) in the mammary tissue had been used to quantify lipid peroxidation. The tissue TBARS (mammary) were assessed using the Ohkawa et al. method [18].

2.6.2 Assessment on antioxidant enzymes

The concentrations of enzymatic antioxidants such as superoxide dismutase (SOD), catalase (CAT), and glutathione peroxidase (GPx) were assessed using Kakkar et al. [19], Sinha et al. [20] and Rotruck et al. [21] techniques, whereas non-enzymatic antioxidants like reduced glutathione (GSH), vitamin C (Vit-C), and vitamin E (Vit-E) levels in mammary tissue were evaluated using Ellman et al [22], Omaye et al. [23] and Desai et al. [24] techniques.

2.6.3 Assessment on Biotransformation enzymes

The quantities of cytochrome P450 (Cyt-P450) and cytochrome b5 (Cyt-b5) in mammary tissue were evaluated using Omura and Sato [25] procedures. NADPH-cytochrome C reductase was assessed by Phillips and Langdon [26] techniques. The activity of glutathione-S-transferase (GST) in mammary tissue were investigated by Habig et al. [27]. The glutathione reductase (GR) levels in mammary tissues were analyzed by Carlberg and Mannervik [28]. The proportion of DT-diaphorase (DTD) in mammary

tissue was assessed by Ernster's [29] protocol with slight adjustments.

2.6.4 Assessment on lipid profile

Folch et al. [30] approach was used to extract lipids from mammary tissues. Zlatkis et al. [31] kit's technique was used to measure total cholesterol (TC) in mammary tissue. The Foster and Dunn [32] method was used to quantify triglycerides (TG) in mammary tissue. Falholt et al. [33] approach was used to measure the free fatty acid content acid (FFA) in mammary tissue. The Zilversmit and Davis [34] method was used to determine phospholipid (PL) levels in mammary tissue.

2.7 Mammary Histology

The mammary tissue of both control and experimental rats was dissected, preserved in neutral buffered formalin (10 % formaldehyde), dehydrated using ethanol solutions, and then embedded in paraffin wax. Tissues were sliced to a thickness of 3-5 μm and stained with Mayer's haematoxylin and eosin (H&E). Haematoxylin and eosin stain for standard observation to visualize tissue microanatomy. Additionally, toluidine blue (TB) staining was used to evaluate the population of mast cells and periodic acid schiff's staining is used to indicate the existence of polysaccharides. The light electric microscope (40x) was then used to conduct further examinations [35].

2.8 Immunohistochemistry

The tissue sections were deparaffinized by heating them at 60°C for 10 minutes, accompanied by 3 xylene rinses. After been gradually hydrated with graded alcohol, the slides were then incubated in citrate buffer (pH 6.0) in a microwave oven for two cycles of 5-minute periods for antigen retrieval. After cooling for 20 minutes, the sections were rinsed with Tris-buffered saline (TBS) and washed with 3 % H_2O_2 in Dis. H_2O for 15 minutes to block endogenous peroxidase reaction. Through incubating the sections for 20 minutes with standard goat serum, non-specific antibody binding was minimized. The sections had been then incubated for 1 hour at Room Temperature (RT) with mouse monoclonal antibodies (AhR and Nrf-2). The slides were rinsed with TBS before being incubated for 30 minutes at RT with anti-rabbit/mouse biotin-labeled secondary antibodies, backed up with streptavidin-biotin-

peroxidase. The immune precipitate was stained with 3,3'-diaminobenzidine and counterstained with hematoxylin. The key antibody was substituted with TBS for negative controls. For positive controls, each antibody was run at the same time [36].

2.9 Molecular Docking Studies

Molecular docking studies were accomplished by utilizing Auto dock software in the auto dock 4.2.6 package. The 3-D structures of the protein targets were retrieved from the Protein Data Bank (PDB) using their PDB IDs, such as AhR (4M4X) and Nrf-2 (3WN7). The DG structure was obtained from the PubChem compound database with the PubChem CID: 99474. Following the protein and ligand preparation, the receptor grid generation of and the docking of ligands were also performed. The Biovia Discovery studio Visualizer were used to uncover the mode of binding by picturing the 2D and 3D interactions and analysing such interactions by visualizing all of the specific amino acid residues that interacts in the binding [37].

2.10 Statistical Analysis

A statistical analysis was performed using SPSS V26.0 (IBM SPSS, USA) software package. The data were expressed as mean \pm standard deviation (SD). One way analysis of variance (ANOVA) followed by Tukey's post-hoc test was used to correlate the difference between the variables. A value of $P < 0.05$ was considered statistically significant.

3. RESULTS

3.1 Impact of DG@CS-NP on Carcinogenic Parameters

Table 1 portrays the carcinogenic parameters like tumor incidence, cumulative numbers of tumors, and tumor volume of both the control and cancer bearing animals. This assessment revealed 100 % tumor incidence in DMBA administered rats (Group II). As compared to DMBA-induced rats (Group II), tumor treated rats with DG 10mg/kg b.wt (Group III) and DG@CS-NP 5mg/kg b.wt (Group IV) reported 50% and 16% significantly lower tumor volume and incidence. When contrasted with control cohort rats (Group I), no discrepancies were recorded in

solely addressed Free DG@NP (Group VI) rats. Therefore, DG@CS-NP 5mg/kg b.wt suppressed tumor volume more productively than DG 10mg/kg b.wt.

3.2 Biochemical Findings

3.2.1 Impact of DG@CS-NP on lipid peroxidative marker

Fig. 1. presented the concentrations of lipid peroxidative marker (TBARS) in mammary tissues of both the control and experimental rats. DMBA administered rats (Group II) displays significantly elevated levels of TBARS than control rats (Group I). Oral administration of DG 10mg/kg b.wt (Group III) and DG@CS-NP 5mg/kg b.wt (Group IV) significantly diminished TBARS levels when compared with DMBA-induced rats (Group II). In addition to this, CS-NP 5mg/kg b.wt (Group V) orally treated rats also express no significant variations on contrast with DMBA-induced rats (Group II). However, no significant alterations were observed in free DG@NP (Group VI) alone treated rats when compared with control rats (Group I). In terms of limiting TBARS levels, DG@CS-NP 5mg/kg b. wt was proven to be more active than DG 10mg/kg b.wt.

3.2.2 Impact of DG@CS-NP on antioxidant enzymes

Fig. 2. indicate the levels of mammary tissue enzymatic antioxidants (SOD, CAT, and GPx) and non-enzymatic antioxidants (GSH, Vit C, and Vit E) in both control and experimental group animals. SOD, CAT, GPx, GSH, Vit C, and Vit E levels significantly lower in DMBA-induced rats (Group II) when compared with control rats (Group I). Fortunately, oral administration of DG 10mg/kg b.wt (Group III) and DG@CS-NP 5mg/kg b.wt (Group IV) depicts significantly escalated levels of SOD, CAT, GPx, GSH, Vit C, and Vit E on compared with DMBA rats (Group II). When CS-NP 5mg/kg b.wt (Group V) treated rats were compared to DMBA group rats (Group II), no variations were noted. Despite this, no significant differences were recorded in Free DG@NP (Group VI) alone treated rats when compared to control rats (Group I). In terms of antioxidant levels, DG@CS-NP 5mg/kg b.wt was reported to be quite active than DG 10mg/kg b.wt.

Table 1. Impact of DG@CS-NP on tumor incidence, total number of tumors and tumor volume in control and experimental rats

Groups	Tumor incidence (%)	Number of tumors (N)	Tumor volume (mm ³ /rat)
I	-	-	-
II	100%	(6)/6	22.14±2.76
III	50%	(3)/6	12.41±1.37 ^{***}
IV	16%	(1)/6	4.34±0.63 ^{***}
V	100%	(6)/6	22.04±2.26
VI	-	-	-

Tumor volume was measured using the formula $V = 4/3\pi (D1/2) (D2/2) (D3/2)$, where D1, D2 and D3 are the three diameters (in mm) of the tumor; (N) indicates total number of rats bearing tumors. Values are expressed as mean ± SD for six rats in each group. Significant levels are ^{***}P < 0.001 when compared with DMBA group

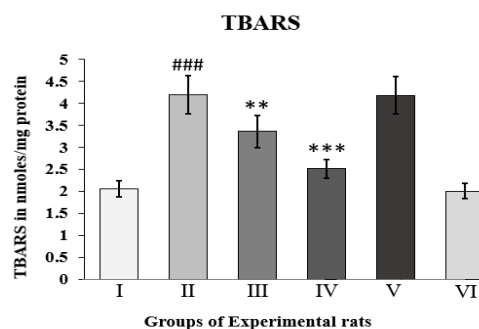


Fig. 1. Impact of DG@CS-NP on the proportions of lipid peroxidative marker (TBARS) in the mammary tissue of control and experimental rats

TBARS: μmol of MDA released per microgram of protein per minute; Values are expressed as mean ± SD for six rats in each group; Significant levels are ^{###}P < 0.001 when compared with control group and ^{**}P < 0.01, ^{***}P < 0.001 when compared with DMBA group

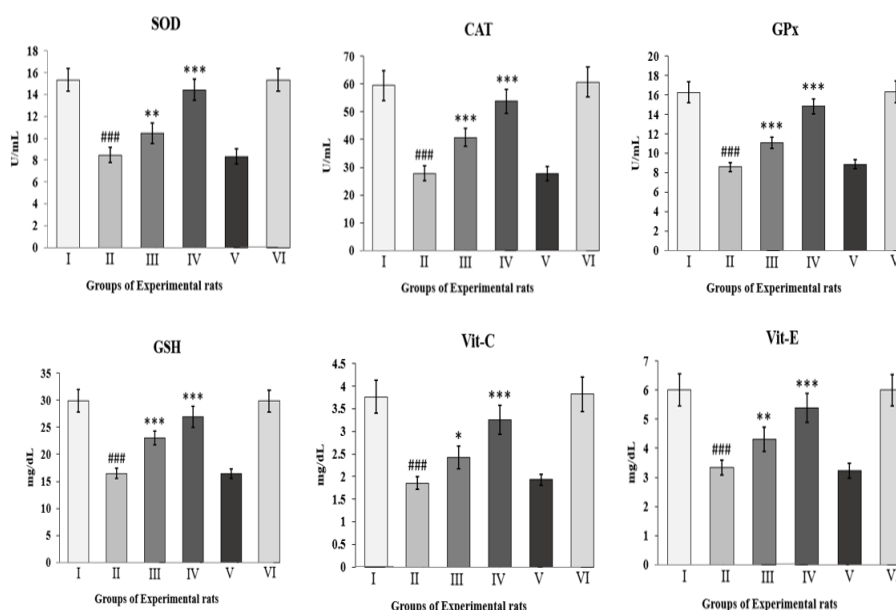


Fig. 2. Impact of DG@CS-NP on the quantities of enzymatic antioxidants (SOD, CAT, and GPx) and non-enzymatic antioxidants (GSH, Vit C, and Vit E) in the mammary tissue of control and experimental rats

SOD: U: Amount of enzyme to inhibit 50% NBT reduction/min; CAT: U: μmol of H₂O₂ consumed/min; GPx: U: μg of GSH consumed/min; Values are expressed as mean ± SD for six rats in each group. Significant levels are ^{###}P < 0.001 when compared with control group and ^{*}P < 0.5, ^{**}P < 0.01, ^{***}P < 0.001 when compared with DMBA group

3.2.3 Impact of DG@CS-NP on Biotransformation enzymes

Fig. 3. displays the concentrations of phase I (Cyt P450, Cyt-b5, Cyt-C) and phase II (GST, GR, and DTD) biotransformation enzymes in both control and experimental rats mammary microsomes. The concentrations of Cyt P450, Cyt-b5 and Cyt-C were significantly elevated, while the GST, GR and DTD concentrations significantly diminished in DMBA induced cancer bearing rats (Group II) when compared with the control group rats (Group I). Contrasted with DMBA (Group II) rats, oral administration of DG 10mg/kg b.wt (Group III) and DG@CS-NP 5mg/kg b.wt (Group IV) exhibit significantly reduced Cyt P450, Cyt-b5 and Cyt-C enzymes with escalated GST, GR, and DTD enzymes. While CS-NP 5mg/kg b.wt (Group V) treated rats were compared to DMBA (Group II) rats, no modifications were identified. Conversely, Free DG@NP (Group VI) alone administered rats indicates no significant differences in the amounts of biotransformation enzymes when compared to control rats (Group I). It was

unearthed that DG@CS-NP 5mg/kg b.wt was more robust than DG 10mg/kg b.wt on regulating detoxification enzymes.

3.2.4. Impact of DG@CS-NP on lipid profile

Fig. 4. reveals the ratio of lipid profile (TG, TC, PL, FFA) in the mammary tissue of both control and experimental rats. DMBA-administered rats (Group II) have notably increased lipid profiles than control rats (Group I). Oral dosing of DG 10mg/kg b.wt (Group III) and DG@CS-NP 5mg/kg b.wt (Group IV) greatly reduced TG, TC, PL, and FFA content in contrast to DMBA-induced rats (Group II). Conversely, CS-NP 5mg/kg b.wt (Group V) orally treated rats display no significant changes when compared to DMBA-induced rats (Group II). Likewise, there were no substantial changes among free DG@NP (Group VI) alone treated rats and control rats (Group I). Finally, DG@CS-NP 5mg/kg b.wt was evidenced to be more proactive in regulating lipid profile levels than DG 10mg/kg b.wt.

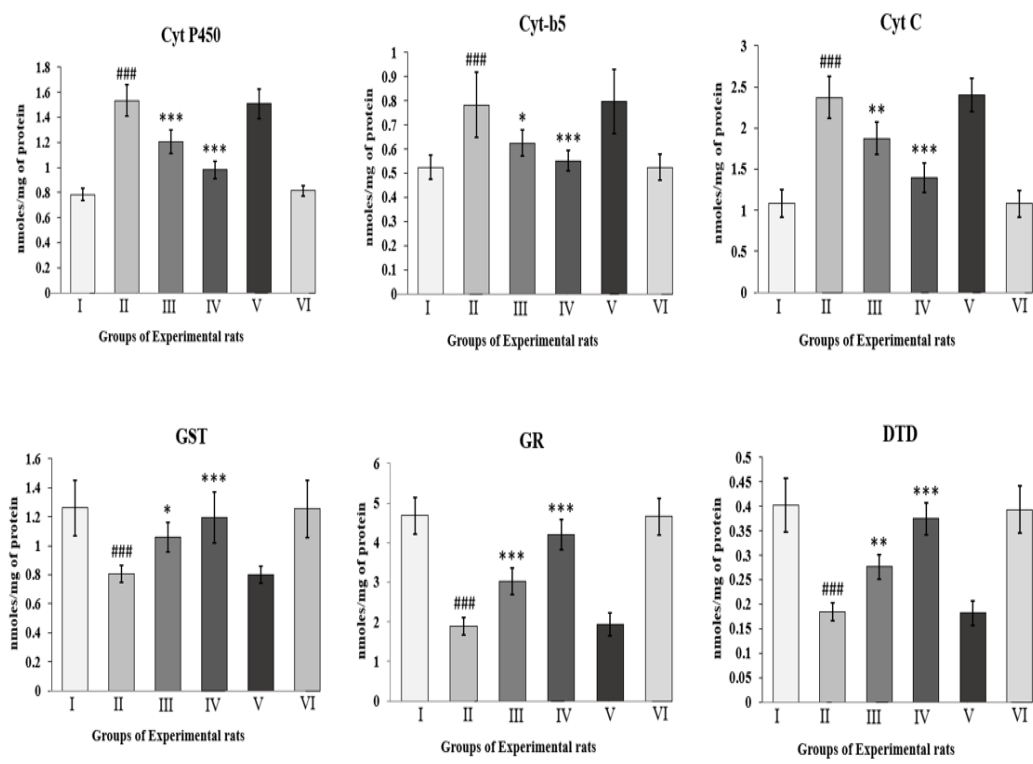


Fig. 3. Impact of DG@CS-NP on the proportions of phase I (Cyt P450, Cyt-b5 and Cyt-c) and phase II (GST, GR, and DTD) biotransformation enzymes in the mammary tissue of control and experimental rats.

Values are expressed as mean \pm SD for six rats in each group. Significant levels are ###P < 0.001 when compared with control group and *P < 0.05, **P < 0.01, ***P < 0.001 when compared with DMBA group.

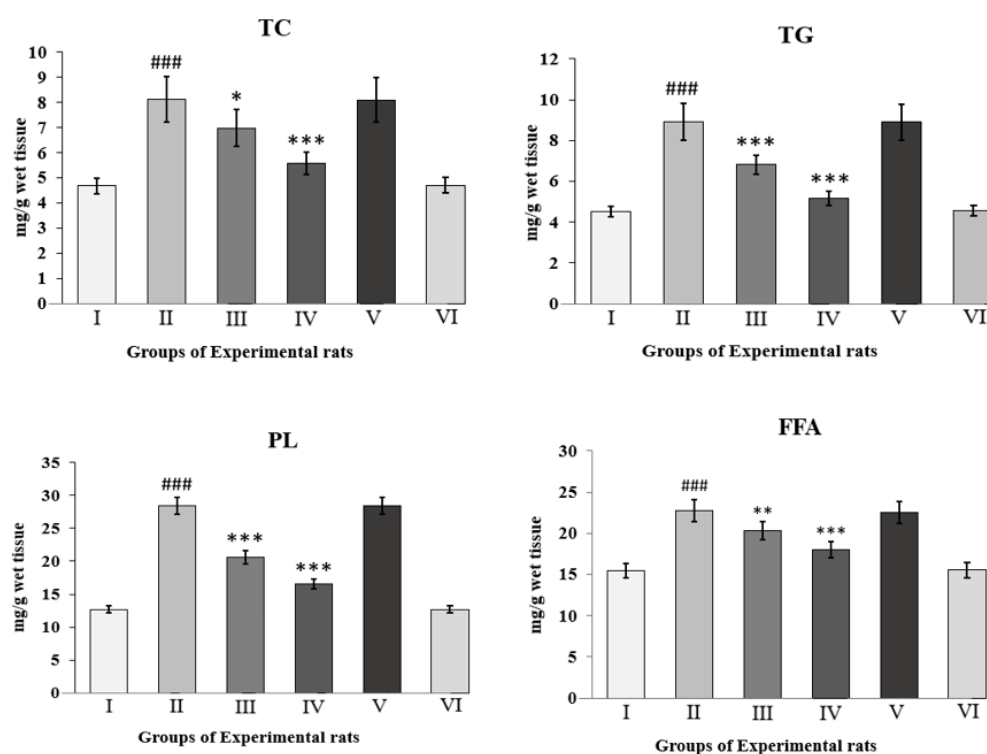


Fig. 4. Impact of DG@CS-NP on the quantities of lipid profile markers (TG, TC, PL, FFA) in the mammary tissue of control and experimental rat

Values are expressed as mean \pm SD for six rats in each group. Significant levels are #### $P < 0.001$ when compared with control group and * $P < 0.05$, ** $P < 0.01$, *** $P < 0.001$ when compared with DMBA group.

3.3 Histopathological Findings

3.3.1 Haematoxylin and eosin staining

Histopathological alterations in mammary tissue sections of control and experimental rats were depicted in Fig. 5 (A–F). The mammary tissue morphology of control rats (Group I) (A) and Free DG@NP (Group VI) (F) alone treated rats appeared normal. In contrast, rats administered with DMBA (Group II) (B) and CS-NP 5mg/kg b.wt (Group V) (E) exhibited invasive ductal carcinoma with aberrant cellular proliferation. Substantial ductal hyperplasia and modest tumor infiltration have been detected in DG 10mg/kg b.wt (Group III) (C) treated rats. The ductal architecture was almost normal in DG@CS-NP 5mg/kg b.wt (Group IV) (D) medicated rats. It was reported that DG@CS-NP 5mg/kg b.wt was more potent than DG 10mg/kg b.wt.

3.3.2 Toluidine blue staining

Toluidine blue staining analysis on mast cell population in mammary tissues of control and experimental rats were displayed in Fig. 6 (A–F). When DMBA-induced animals (Group II) (B) were compared with control rats (Group I) (A),

the mast cell population was dramatically increased. On contrast to DMBA-induced rats (Group II) (B), oral dosage of DG 10mg/kg b.wt (Group III) (C) and DG@CS-NP 5mg/kg b.wt (Group IV) (D) drastically decreased the rates of mast cell population. While comparing CS-NP 5mg/kg b.wt (Group V) (E) treated rats to DMBA induced rats (Group II), no changes were noted (B). Likewise, comparing Free DG@NP (Group VI) (F) alone treated animals with control rats (Group I), no alterations were spotted (A). Evidently, DG@CS-NP 5mg/kg b.wt was displayed to be more effective than DG 10mg/kg b.wt at suppressing mast cell population.

3.3.3 Periodic acid Schiff's staining

The PAS staining assessment on glycoprotein in mammary tissues of control and experimental rats has been shown in Fig. 7. (A–F). When DMBA-induced animals (Group II) (B) were compared to control rats (Group I) (A), glycoprotein tiers were dramatically elevated. As contrast with DMBA-induced rats (Group II) (B), dosage of DG 10mg/kg b.wt (Group III) (C) and DG@CS-NP 5mg/kg b.wt (Group IV) (D) drastically decreased the scores of glycoproteins. While comparing CS-NP 5mg/kg b.wt (Group V)

(E) treated rats with DMBA induced animals (Group II) (B), no alterations were observed. Likely, when comparing control rats (Group I) (A) with Free DG@NP (Group VI) (F) alone treated rats, no changes were seen. Consequently, DG@CS-NP 5mg/kg b.wt was proven to be more effective than DG 10mg/kg b.wt at lowering glycoprotein aggregation.

3.4 Immunohistochemical Findings

Fig. 8 shows the immunohistochemical expression of AhR in the mammary tissues of

both the control and experimental rats. The expression of AhR were elevated in DMBA-induced rats (Group II and V) with ductal structures exposing noted focal inflammations. Inversely, the AhR expression were diminished in DG 10mg/kg b.wt and DG@CS-NP 5mg/kg b.wt (Group III and IV), showing moderate inflammation in Group III, while posing ductal structures with no evidence of inflammation, fibrosis, and malignancy in Group IV. Whereas control rats (Group I and VI) show normal AhR expressions.

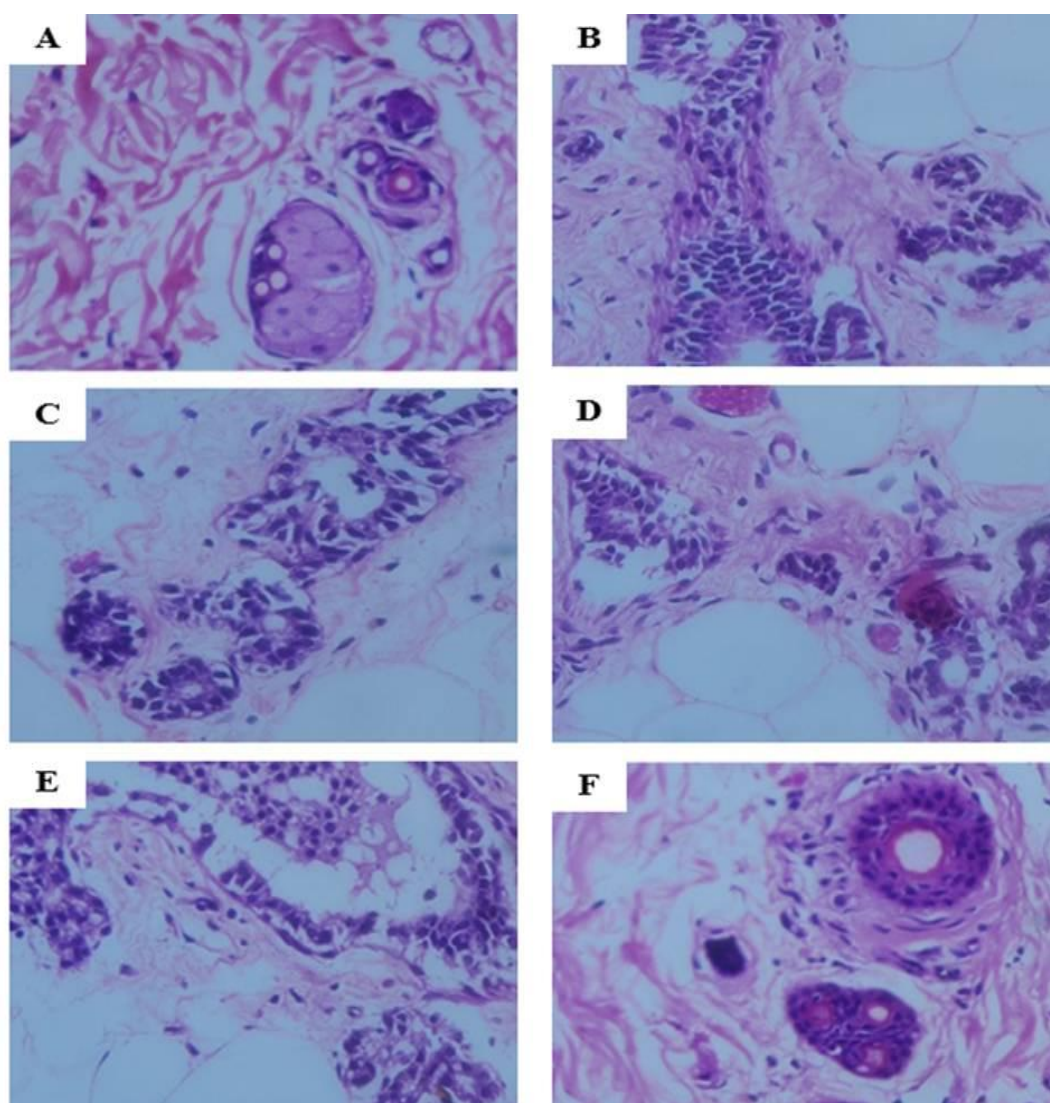


Fig. 5. Impact of DG@CS-NP on histopathological alterations of mammary tissue in control and experimental rats

Histology on mammary tissues of control (A) and Free DG@NP (F) alone treated rats showed normal architecture of mammary tissue; Mammary tissues of DMBA induced (B) and CS-NP 5mg/kg b.wt(E) treated rats showed invasive ductal carcinoma; Mammary tissues of DG10mg/kg b.wt (C) treated rats showed moderate ductal hyperplasia and mild tumor infiltration; Mammary tissues of DG@CS-NP 5mg/kg b.wt (D) treated rats showed almost near normal ductal architecture

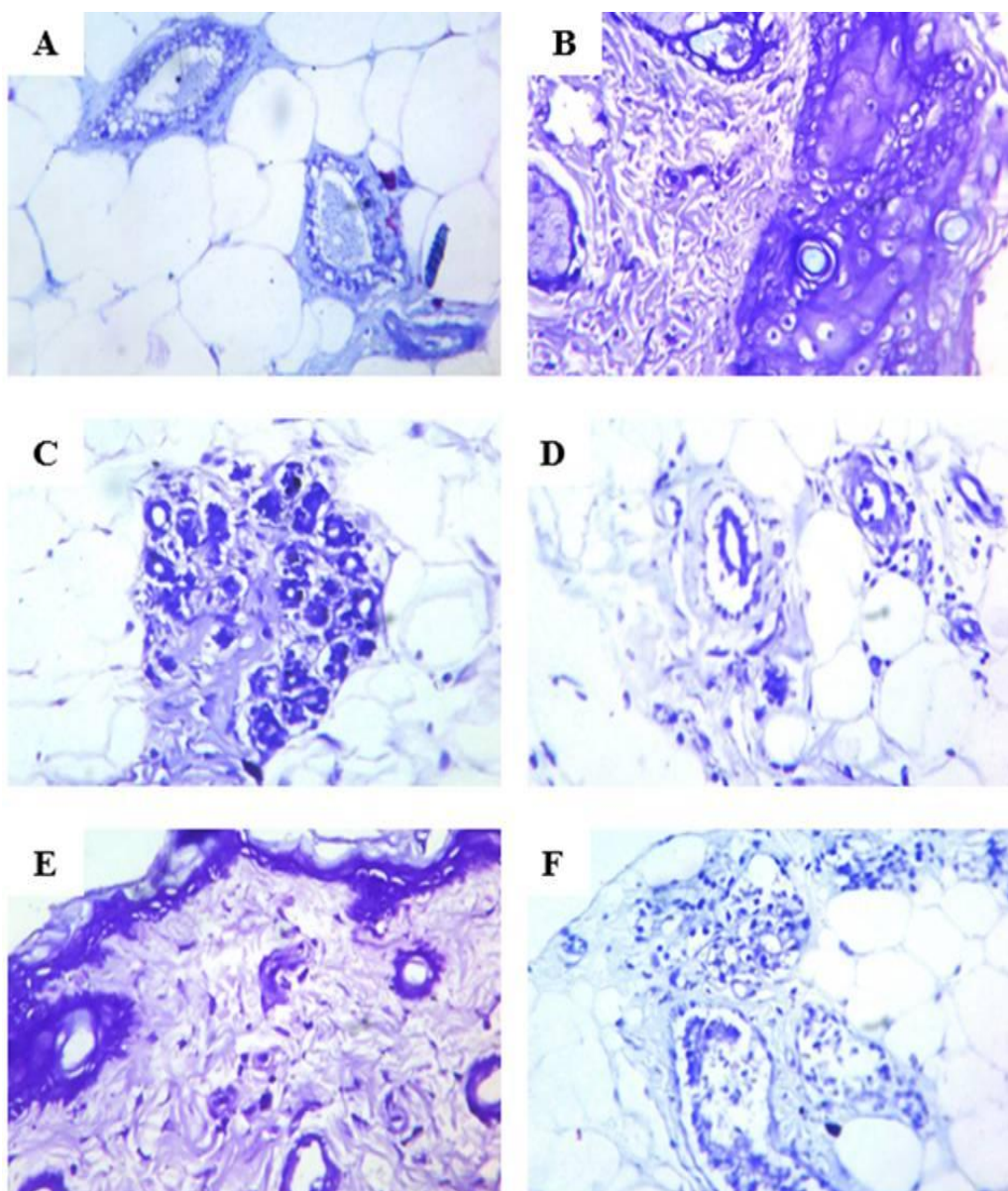


Fig. 6. Impact of DG@CS-NP on histopathological analysis of mast cell population in the mammary tissues of control and experimental rats

Histochemical analysis on mammary tissues of control (A) and Free DG@NP (F) alone treated rats showed normal mammary tissue staining; Mammary tissues of DMBA induced (B) and CS-NP 5mg/kg b.wt (Group V) (E) treated rats showed elevated levels of mast cell population; Mammary tissues of DG 10mg/kg b.wt (C) and DG@CS-NP 5mg/kg b.wt (D) orally treated rats showed decreased levels of mast cell population as compared to DMBA induced cancer bearing rats(B).

Fig. 9 shows the immunohistochemical expression of Nrf-2 in the mammary tissues of both the control and experimental rats. The expression of Nrf-2 was diminished in DMBA-induced rats (Group II and V) with ductal structures exposing noted focal inflammations. Inversely, the Nrf-2 expressions were escalated in DG 10mg/kg b.wt and DG@CS-NP 5mg/kg

b.wt (Group III and IV), showing moderate inflammation in Group III, while posing ductal structures with no evidence of inflammation, fibrosis, and malignancy in Group IV. Whereas control rats (Group I and VI) show normal Nrf-2 expressions. As an outcome, DG@CS-NP 5mg/kg b.wt was proven to be more active than DG 10mg/kg b.wt in all scenarios.

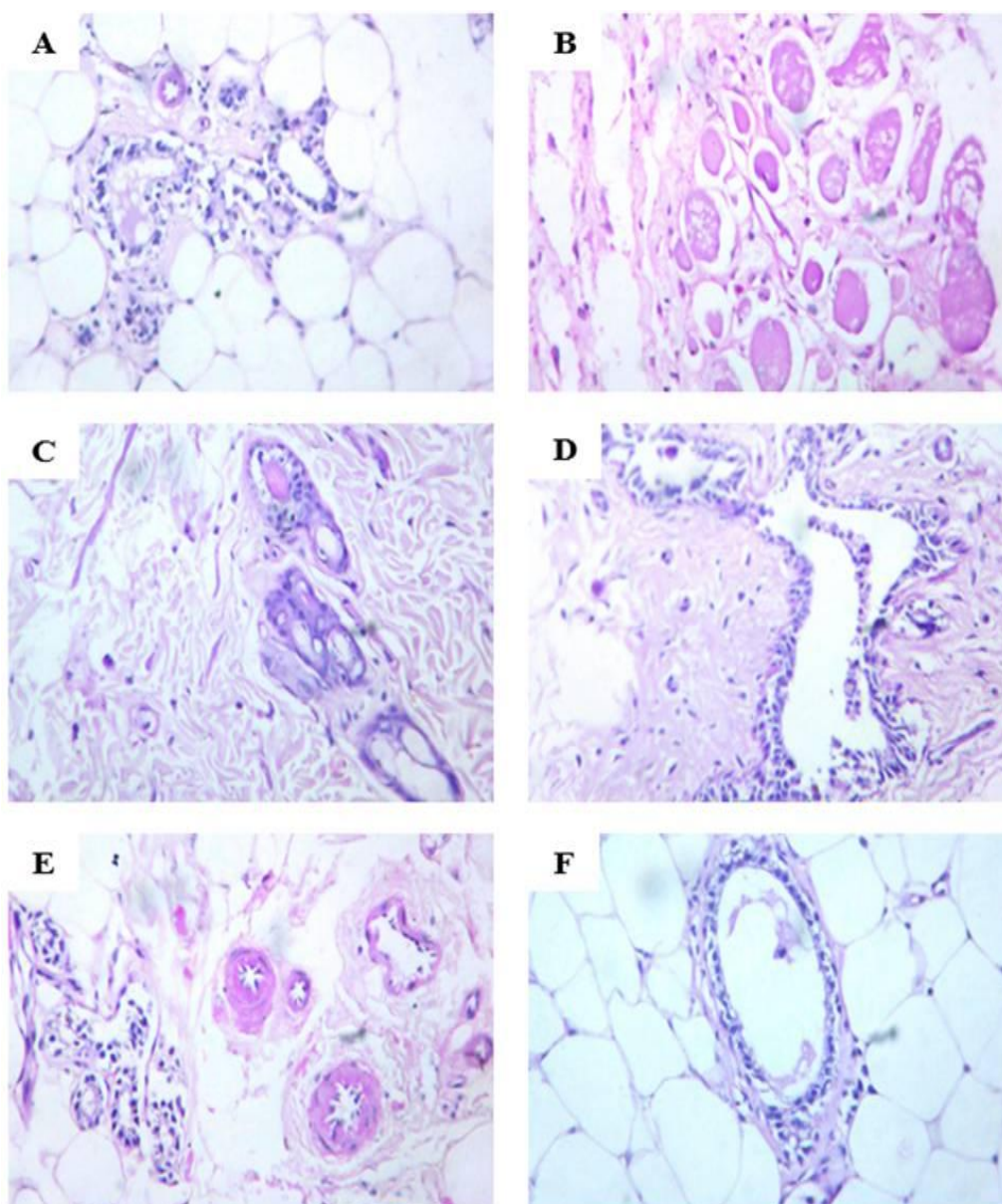


Fig. 7. Impact of DG@CS-NP on histopathological analysis of PAS staining in mammary tissue of control and experimental rats

Histopathological analysis of PAS staining in mammary tissue of control and experimental rats (A-F). Control (A) and Free DG@NP (F) alone treated rats showed normal mammary tissue staining. DMBA induced (B) and CS-NP 5mg/kg b.wt (E) treated rats showed increased levels of glycoprotein. DG10mg/kg b.wt (C) and DG@CS-NP 5mg/kg b.wt (D) treated rats showed decreased levels of glycoprotein as compared to DMBA induced cancer bearing rats (B).

3.5 Molecular Docking Findings

To validate Diosgenin's interactions with core target signaling kinases (AhR and Nrf-2) we employed computational docking techniques to pinpoint docking spots. Molecular docking investigations proved that diosgenin binds with both the catalytic domains of AhR and Nrf-2. As displayed in Fig. 10, the DG-AhR complex

possesses a strong binding energy of -8.91 kcal/mol featuring active interaction residues Trp174, Ala 207, Met210, Tyr239, Pro255, and Leu257. Additionally, DG with Nrf-2 has a binding energy of -11.35 kcal/mol with vital residues Val 606, Ala 607, Val 608, Ala 366, Cys 368, Arg 415, and Val 418. Moreover, such outcomes are well congruent with immunohistochemical responses.

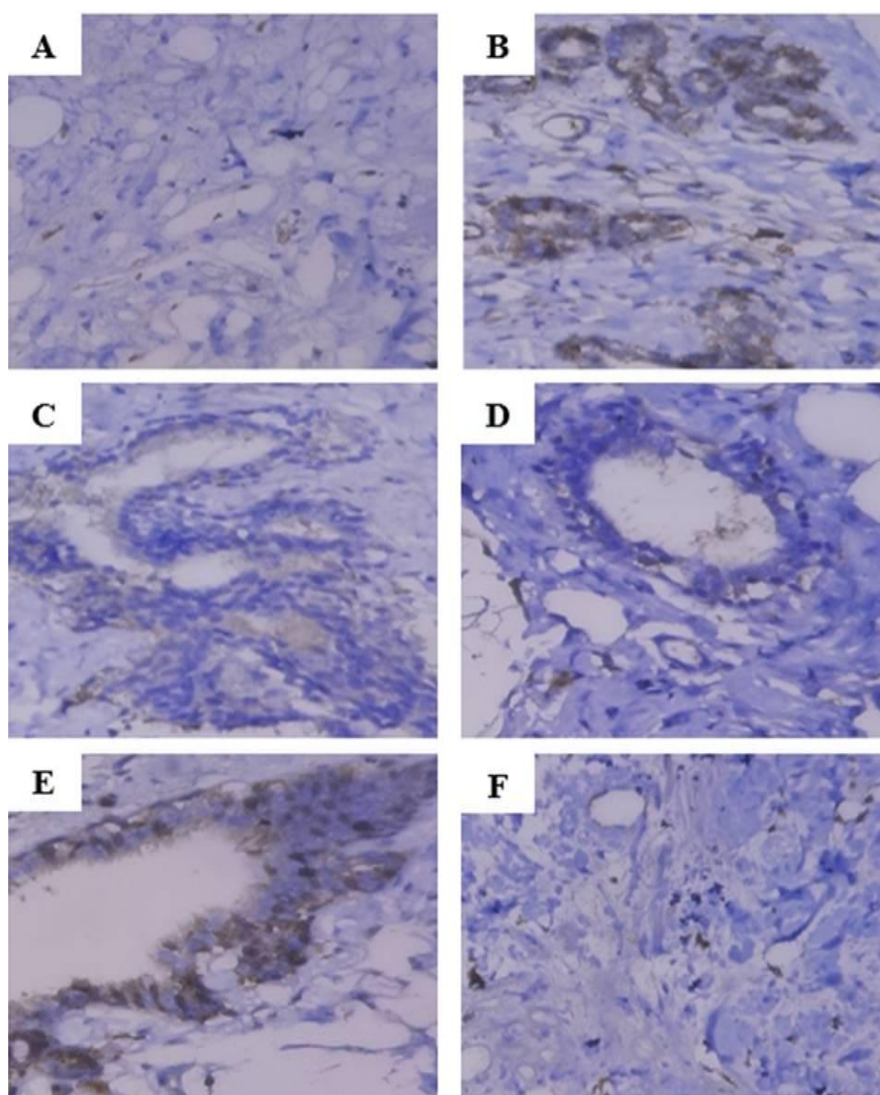


Fig. 8. Immunohistochemical analysis of AhR expression in the mammary tissues of control and experimental rats

Immunohistochemical on mammary tissues of control (A) and Free DG@NP (F) alone treated rats showed normal mammary tissue staining; Mammary tissues of DMBA induced (B) and CS-NP 5mg/kg b.wt (E) treated rats showed increased expression of AhR; Mammary tissues of DG10mg/kg b.wt (C) and DG@CS-NP 5mg/kg b.wt (D) orally treated rats showed diminished expression AhR of as compared to DMBA induced cancer bearing rats (B).

4. DISCUSSION

Breast cancer represents a fatal human health challenge in such a global arena. It is a compendium of biochemical and histopathological alterations which emerged within the mammary gland. These biochemical signs alarm the cancerous root meristem [38]. Existing pharmaceuticals that are meeting therapeutic rejections might be linked to mistargeting core trait which underlies all of the biochemical abnormalities cited in the cancerous

progression [39]. Presently, the phyto encapsulated nanocarrier system delivers multiple improvements in the treatment of chronic cancer via site-specific and target-oriented dispatch of precise pharmaceuticals into the mechanistic biochemical site with zero negative effects [40]. Therefore, in order to address multiple biochemical targets, we fabricate diosgenin encapsulated chitosan nanoparticle (DG@CS-NP) to restore such biochemical changes in DMBA induced rat mammary carcinogenesis.

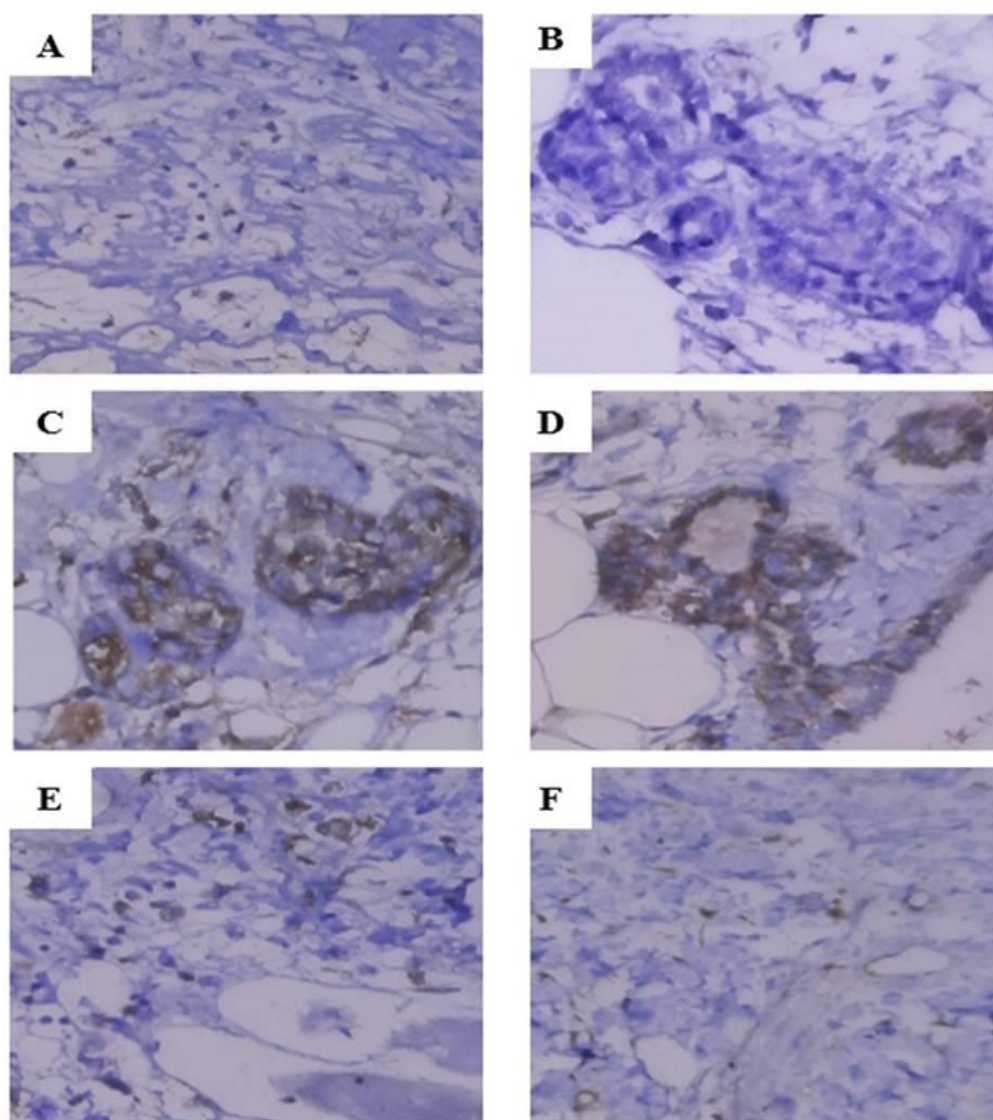


Fig. 9. Immunohistochemical analysis of Nrf-2 expression in the mammary tissues of control and experimental rats

Immunohistochemical on mammary tissues of control (A) and Free DG@NP (F) alone treated rats showed normal mammary tissue staining; Mammary tissues of DMBA induced (B) and CS-NP 5mg/kg b.wt (E) treated rats showed decreased expression of Nrf-2; Mammary tissues of DG10mg/kg b.wt (C) and DG@CS-NP 5mg/kg b.wt (D) orally treated rats showed elevated expression Nrf-2 of as compared to DMBA induced cancer bearing rats(B).

DMBA, an exotic chemical carcinogen metabolically provoked via activating AhR, which evokes phase I enzyme (Cyt P450, Cyt-b5 and Cyt-c) synthesis. Activated AhR cleaves and rides into the nucleus, thereby dimerize with ARNT and connect to xenobiotic-responsive elements in the promoter region to enhance their gene expression [41]. Thereby, it emits a multitude of free radicals by raising oxidative stress inside the cellular environment. The oxidative stress aggregation triggers an

extensive enhancement in the cellular reduction potency that may lead to a declined strength of the balance between redox pairs. Cellular and organelle frameworks are incredibly sensitive to ROS damage culminating in lipid peroxidation with elevated levels of TBARS [42]. Moreover, cancerous cells were invariably subjected to a biologically demanding environment with scarce oxygen and nutrient supply. Such stress alters the equilibrium of intrinsic production and extrinsic consumption of fatty acids, which cells

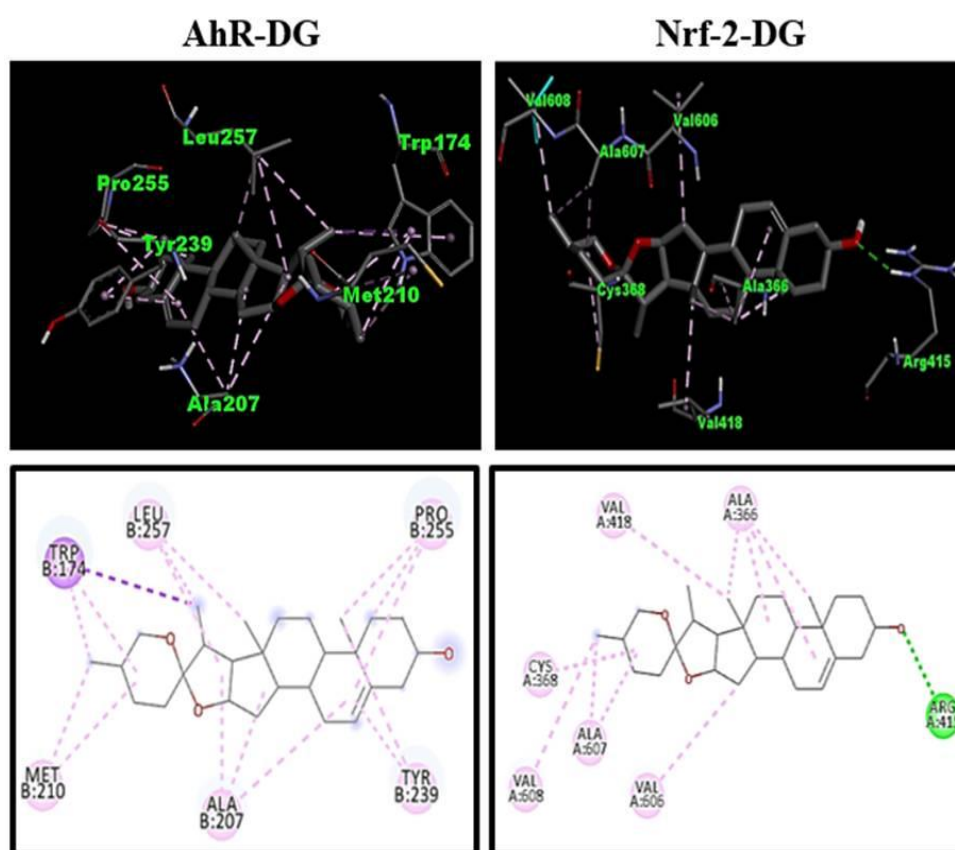


Fig. 10. Molecular docking analysis of DG interactions with AhR and Nrf-2 proteins

require for cellular biosynthesis, energy generation, and protein modulation. These modifications might impact the demand of functional lipids for membrane composition and the formulation and deterioration of lipids that lead to imbalanced energy homeostasis. Consequently, enhanced fatty acid and cholesterol biogenesis, and the metabolism of free fatty acids via triacyl glycerides, can result in an escalated lipid grades which have altered signaling features in multiple facets of carcinogenesis [43]. As it is evident that, countless research has revealed that DMBA-induced experimental rat mammary carcinomas disrupt tissue redox equilibrium, thus signaling in oxidative damage which elicits varied biochemical and pathological abnormalities [44]. As a consequence, silencing lipid peroxidation seems to be the possible mechanistic pathway in combating mammary carcinogenesis. Our study highlighted the marginalization of the lipid peroxidative marker TBARS with a diminished level of phase-I enzymes and reduced lipid profile in DG@CS-NP medicated rats via abrogating AhR ligand activation.

AhR deactivation can be achieved by activating the Nrf-2 ligand. Nrf2, a transcription factor influences cellular defenses against inflammatory and oxidative threats by restricting the expressions of genes engaged in oxidative stress and drug detoxification. Activated Nrf2 detaches from Keap1, runs into the nucleus and dimerizes with Maf or c-Jun. Then, this heterodimer ties with antioxidant response elements and enables the cells resilient to a chemical carcinogen (DMBA) by regulating the function of numerous phase I and II drug-metabolizing enzymes [45]. Its stimulation has also emerged as a massive root mechanism for numerous noted oxidative stress modulators such as enzymatic (SOD, CAT, and GPx) and non-enzymatic (GSH, Vit C, and Vit E) anti-oxidants. Although enzymatic antioxidants operate by turning the oxidized metabolic substances to hydrogen peroxide (H_2O_2) followed by reducing it to water by a multi-step mechanism with cofactors like iron, zinc, copper, and manganese. The non-enzymatic antioxidants directly interrupt and stop the free radical chain reactions. These antioxidant modules can constrain ROS peaks by influencing altered gene expression and associated

signaling pathways in order to retain redox balance and cellular component integrity [46]. These therapeutic mechanisms have well been detected in our outcomes. Orally administering Nrf2-ARE activator DG@CS-NP visibly elevates the enzymatic (SOD, CAT, and GPx) and non-enzymatic (GSH, Vit C, and Vit E) anti-oxidants with an escalated level of phase II (GST, GR, and DTD) drug-metabolizing enzymes. Molecular docking studies also support the active interaction of DG with AhR and Nrf2, the central instigators and a pivotal controller of the cellular defenses towards xenobiotic and oxidative stress response in rat mammary carcinoma.

5. CONCLUSION

To conclude, DMBA-induced upregulation of phase-I carcinogen metabolizing enzymes were driven by AhR, results in ROS overproduction, triggered via metabolism of carcinogen/xenobiotic promotes lipid peroxidation, alterations in mammary cell structure, and downregulation of Nrf2 actions, signifying a drop in the initiation of phase II enzyme synthesis. Therefore, Diosgenin encapsulated nanocarrier system actively targets the key mechanisms in scavenging various physiological radical reactions. Thus, DG@CS-NP actively normalizes the biochemical and histopathological alterations in DMBA induced rat mammary carcinoma via attenuating the AhR-Nrf-2 signalling cascades. Hence, such core mechanisms open up the path for DG@CS-NP as a potent drug molecule in breast cancer mitigation.

CONSENT

It is not applicable.

ETHICAL APPROVAL

This study protocol was approved by the Institutional Animal Ethics Committee (IAEC), regulated by the Committee for the Purpose of Control and Supervision of Experiments on Animals (CPCSEA), New Delhi, India. (Proposal No. 1241, dated April 23, 2019).

DISCLAIMER

The products used for this research are commonly and predominantly use products in our area of research and country. There is absolutely no conflict of interest between the authors and

producers of the products because we do not intend to use these products as an avenue for any litigation but for the advancement of knowledge. Also, the research was not funded by the producing company rather it was funded by personal efforts of the authors.

ACKNOWLEDGEMENT

The authors would like to thank the Department of Biochemistry and Biotechnology, Annamalai University for providing the research facilities and support. The authors would also like to thank Central Animal House, Rajah Muthiah Medical College, and Hospital, Annamalai University for animal maintenance facilities.

COMPETING INTERESTS

Authors have declared that no competing interests exist.

REFERENCES

1. Sharma K, Costas A, Shulman LN, Meara JG. A systematic review of barriers to breast cancer care in developing countries resulting in delayed patient presentation. *J Oncol*. 2012;1(1):1-8.
2. Vinothini G, Murugan RS, Nagini S. Evaluation of molecular markers in a rat model of mammary carcinogenesis. *Oncol Res: Preclin Clin Cancer Ther*. 2009; 17(10):483-93.
3. Angeline Kirubha SP, Anburajan M, Venkataraman B, Akila R, Sharath D, Raj B. Evaluation of mammary cancer in 7, 12-dimethylbenz (a) anthracene-induced wister rats by asymmetrical temperature distribution analysis using thermography: A comparison with serum Cea levels and histopathology. *J Biomed Biotech*. 2012;1(1):1-11.
4. Maayah ZH, Ghebeh H, Alhaider AA, El-Kadi AO, Soshilov AA, Denison MS, Ansari MA, Korashy HM. Metformin inhibits 7, 12-dimethylbenz [a] anthracene-induced breast carcinogenesis and adduct formation in human breast cells by inhibiting the cytochrome P4501A1/aryl hydrocarbon receptor signaling pathway. *Toxicol Appl Pharmacol*. 2015;284(2):217-26.
5. Han EH, Hwang YP, Jeong TC, Lee SS, Shin JG, Jeong HG. Eugenol inhibit 7, 12-dimethylbenz [a] anthracene-induced genotoxicity in MCF-7 cells: Bifunctional

- effects on CYP1 and NAD (P) H: quinone oxidoreductase. FEBS Lett. 2007;581(4): 749-56.
6. Rajakumar T, Pugalendhi P, Thilagavathi S, Ananthakrishnan D, Gunasekaran K. Allyl isothiocyanate, a potent chemopreventive agent targets AhR/Nrf2 signaling pathway in chemically induced mammary carcinogenesis. Mol Cell Biochem. 2018;437(1):1-2.
 7. Kim YC, Seok S, Byun S, Kong B, Zhang Y, Guo G, et al. AhR and SHP regulate phosphatidylcholine and S-adenosylmethionine levels in the one-carbon cycle. Nat Commun. 2018;9(1):1-3.
 8. Dietrich C. Antioxidant functions of the aryl hydrocarbon receptor. Stem cells Int. 2016;1(1):1-10.
 9. Cort A, Ozben T, Saso L, De Luca C, Korkina L. Redox control of multidrug resistance and its possible modulation by antioxidants. Oxid Med Cell Longev. 2016;11(1):1-17.
 10. Isah T. Stress and defense responses in plant secondary metabolites production. BiolRes. 2019;52(39):1-25.
 11. Li YN, Guo Y, Xi MM, Yang P, Zhou XY, Yin S, et al. Saponins from *Aralia taibaiensis* attenuate D-galactose-induced aging in rats by activating FOXO3a and Nrf2 pathways. Oxid Med Cell Longev. 2014;3(1):1-13.
 12. Mirunalini S, Shahira R. Novel effect of diosgenin—a plant derived steroid. A review. Pharmacol Online. 2011;1(1):726-36.
 13. Manobharathi V, Mirunalini S. Pharmacological characteristics of a phyto steroidal food saponin: Diosgenin. Afr J BiolSci. 2020; 2 (2), 77-87.
 14. Arulmozhi V, Pandian K, Mirunalini S. Ellagic acid encapsulated chitosan nanoparticles for drug delivery system in human oral cancer cell line (KB). Colloids Surf B: Bioint. 2013; 110(1):313-20.
 15. Isabella S, Mirunalini S. Protective effect of 3, 3'-Diindolylmethane encapsulated chitosan nanoparticles prop up with lipid metabolism and biotransformation enzymes against possible mammary cancer. JAppl Pharm Sci. 2017;7(3):194-201.
 16. Jagadeesan J, Nandakumar N, Rengarajan T, Balasubramanian MP. Diosgenin, a steroidal saponin, exhibits anticancer activity by attenuating lipid peroxidation via enhancing antioxidant defense system during NMU-induced breast carcinoma. JEnv PatholToxicol Oncol. 2012;31(2):121-9
 17. Kumar BP, Puvvada N, Rajput S, Sarkar S, Das SK, Emdad L, et al. Sequential release of drugs from hollow manganese ferrite nanocarriers for breast cancer therapy. JMat Chem B. 2015;3(1):90-101.
 18. Ohkawa H, Ohishi N, Yagi K. Assay for lipid peroxides in animal tissues by thiobarbituric acid reaction. Anal Biochem. 1979;95(2):351-8.
 19. Kakkar, Poonam, Ballabh Das, and P. N. Viswanathan. A modified spectrophotometric assay of superoxide dismutase. Indian J Biochem Biophys.1984;21(2):130-2
 20. Sinha AK. Colorimetric assay of catalase. Anal Biochem. 1972;47(2):389-94.
 21. Jt, Rotruck, Pope AL, Ganther HE, Swanson AB, Hafeman DG, Hoekstra WG. Selenium: biochemical role as a component of glutathione peroxidase. Sci. 1973; 1(1): 588-90.
 22. Ellman GL. Tissue sulfhydryl groups. ArchBiochemBiophys. 1959;82(1):70-7.
 23. Omaye ST, Turnbull JD, Sauberlich HE. Selected methods for the determination of ascorbic acid in animal cells, tissues, and fluids. Methods Enzymol. 1979;62(1):3-11.
 24. Desai ID. Vitamin E analysis methods for animal tissues. Methods Enzymol. 1984; 105(1):138-47.
 25. Omura T, Sato R. The carbon monoxide-binding pigment of liver microsomes I. Evidence for its hemoprotein nature. J Biol Chem. 1964;239(7):2370-8.
 26. Phillips, A.H. and Langdon, R.G., Hepatic triphosphopyridine nucleotide-cytochrome c reductase: isolation, characterization, and kinetic studies. J BiolChem. 1962; 237(8): 2652-2660.
 27. Habig WH, Pabst MJ, Jakoby WB. Glutathione S-transferases the first enzymatic step in mercapturic acid formation. J Biol Chem. 1974;249(22):7130-9.
 28. Carlberg I, Mannervik B. [59] Glutathione reductase. Methods Enzymol. 1985; 113(1): 484-90.
 29. Ernster L. [56] DT diaphorase. Methods Enzymol. 1967; 10(1): 309-17.
 30. Folch J, Lees M, Sloane Stanley GH. A simple method for the isolation and purification of total lipids from animal tissues. J Biol Chem. 1957; 226(1):497-509

31. Zlatkis A, Zak B, Boyle AJ. A method for the direct determination of serum cholesterol. *J Lab Clin Med.* 1953; 41(1):486–92.
32. Foster LB, Dunn RT. Stable reagents for determination of serum triglycerides by a colorimetric Hantzsch condensation method. *Clin Chem.* 1973; 19(1):338–40.
33. Falholt K, Lund B, Falholt W. An easy colorimetric micromethod for routine determination of free fatty acids in plasma. *Clin Chim Acta.* 1973; 46(1):105–11.
34. Zilversmit DB, Davis AK. Microdetermination of plasma phospholipids by trichloro acetic acid precipitation. *J Lab Clin Med.* 1950; 35(1):155–60.
35. Shamsuddin AK, Trump BF. Colon epithelium. II. In vivo studies of colon carcinogenesis. Light microscopic, histochemical, and ultrastructural studies of histogenesis of azoxymethane-induced colon carcinomas in Fischer 344 rats. *J Nat Cancer Ins.* 1981;66(2):389-401.
36. Dantsuka A, Ichii O, Hanberg A, Elewa YH, Otsuka-Kanazawa S, Nakamura T, et al. Histopathological features of the proper gastric glands in FVB/N-background mice carrying constitutively-active aryl-hydrocarbon receptor. *BMC Gastroenterology.* 2019;19(1):1-7.
37. Morris GM, Goodsell DS, Pique ME, Lindstrom WL, Huey R, Forli S. AutoDock 4.2 user guide: The Scripps Research Institute; 2009.
38. Feng Y, Spezia M, Huang S, Yuan C, Zeng Z, Zhang L, et al. Breast cancer development and progression: Risk factors, cancer stem cells, signaling pathways, genomics, and molecular pathogenesis. *Genes Dis.* 2018;5(2):77-106.
39. Jorgenson TC, Zhong W, Oberley TD. Redox imbalance and biochemical changes in cancer. *Cancer Res.* 2013; 73(20):6118-23.
40. Patra JK, Das G, Fraceto LF, Campos EV, del Pilar Rodriguez-Torres M, Acosta-Torres LS, et al. Nano based drug delivery systems: recent developments and future prospects. *JNanobiotech.* 2018;16(1):1-33.
41. Haarmann-Stemmann T, Abel J, Fritsche E, Krutmann J. The AhR–Nrf2 pathway in keratinocytes: on the road to chemoprevention. *J Invest Dermatol.* 2012;132(1):7-9.
42. El-Demerdash, Fatma M., Ehab M. Tousson, Jacek Kurzepa, SamyL Habib. Xenobiotics, oxidative stress, and antioxidants. *Oxid Med Cell Longev.* 2018;1(1):1-2.
43. Munir R, Lisec J, Swinnen JV, Zaidi N. Lipid metabolism in cancer cells under metabolic stress. *Br J Cancer.* 2019; 120(12):1090-8.
44. Batcioglu K, Uyumlu AB, Satilmis B, Yildirim B, Yucel N, Demirtas H, et al. Oxidative Stress in the in vivo DMBA Rat Model of Breast Cancer: Suppression by a Voltage-gated Sodium Channel Inhibitor (RS 100642). *Basic Clin Pharmacol Toxicol.* 2012;111(2):137-41.
45. He F, Ru X, Wen T. NRF2, a transcription factor for stress response and beyond. *Int JMol Sci.* 2020;21(13):1-23.
46. Moussa Z, Judeh ZM, Ahmed SA. Nonenzymatic exogenous and endogenous antioxidants. *Free Rad Med Biol.* 2019;1(1):1-22.

© 2021 Vengaimaran et al.; This is an Open Access article distributed under the terms of the Creative Commons Attribution License (<http://creativecommons.org/licenses/by/4.0>), which permits unrestricted use, distribution, and reproduction in any medium, provided the original work is properly cited.

Peer-review history:
 The peer review history for this paper can be accessed here:
<https://www.sdiarticle4.com/review-history/76135>